

Comparison of LBM-URANS and LBM-VLES for 3D Taylor-Green Vortex Problems

A. Jammalamadaka, Y. Li, R. Zhang and H. Chen
Corresponding author: yanbing.li@3ds.com

Dassault Systemes, 175 Wyman St, Waltham, MA 02451.

Abstract: A Lattice-Boltzmann Method (LBM) based numerical method is applied in this study to solve the time accurate three dimensional flow field of a Taylor-Green vortex (TGV) problem at high Reynolds number. Two turbulence modeling approaches, LBM-RANS/URANS (Unsteady Reynolds-Averaged Navier Stokes) and LBM-VLES (Very Large Eddy Simulation) are investigated. Simulations are performed at Reynolds number of 1600, analysis of temporal evolutions of flow structures, power spectrums and decay rates of kinetic energy, is made on the solutions from the two turbulence models and compared with results from direct numerical simulation (DNS). The comparisons indicated that LBM-RANS approach is over dissipative and cannot capture the vorticity dynamics and evolutions correctly, while the LBM-VLES solution is consistent with data from DNS. Results from TGV simulations at much higher Reynolds numbers ($Re=10^6$) also verified that LBM-VLES is able to capture the right turbulent structures and spectrum scaling laws for the inertial range, while LBM-RANS predicted over damped results.

Keywords: Lattice-Boltzmann Method, Turbulence Modeling, VLES, RANS

1 Introduction

The quality of CFD prediction for complex turbulent flow field is greatly dependent on the underlying closure model for flow turbulence [1,2]. Conventional CFD approaches are based on the closure formulation for the Navier-stokes equations, where the averaged RANS equations or space-filtered equations (LES) are solved. The contributions from either the Reynolds stresses or the Sub Grid Scales (SGS) are approximated based on the model assumptions [1,2]. The most popular linear eddy viscosity type of RANS models uses a linear stress-strain assumption. These models are intrinsically isotropic and were found not suitable for highly unsteady anisotropic turbulent flows [2]. Advanced models such as Reynolds stress model (RSM) or LES has to be used, which increase the model complexity and consequently the computation cost [2].

Lattice Boltzmann method (LBM) is an alternate CFD methodology that solves the Boltzmann equation in its discrete form on a square (or cubic) lattice [3-7]. The LBE has been shown to recover the compressible Navier-Stokes equation at the hydrodynamic limit [3, 4, 8]. In the nearly incompressible limit, it produces the incompressible Navier-Stokes equations with an error proportional to the local Mach number squared. The key advantages in LBM include parallel computation for time dependent flows, ease of modeling various complex fluids, and physical and more straightforward handling of complicated geometries and boundary conditions [6,9,10]. A number of numerical benchmarks have been presented to illustrate the accuracy of LBMs for laminar flows [4, 11]. The LBM-VLES based

turbulence modeling approach has been incorporated into commercial CFD software SIMULIA PowerFLOW[®] and has been demonstrated as a viable and desirable approach for doing very large eddy simulations (VLES) of high Reynolds number turbulent flows in industrial applications [6, 12-15].

The Taylor-Green vortex (TGV) serves as one of the canonical flow problems developed to study the generation of small scales by three-dimensional vortex dynamics and the transition of flow field from well-organized large-scale motion into decaying turbulence [16-23]. It has been chosen in this study to demonstrate the effectiveness of LBM-VLES in predicting three dimensional, unsteady turbulent flows, the results will be directly compared with available LBM based Direct Numerical Simulations (DNS) data and LBM-RANS turbulence model simulation predictions. This paper is organized as follows. First, a description of the studied problem is given (Section 2). Next, some basics of the numerical algorithm and the related turbulence modeling approaches are presented (Section 3). This is followed by the generated results (Section 4) and the conclusions (Section 5).

2 Problem Statement

The three dimensional Taylor-Green vortex flow is a well-documented problem to test the accuracy and the performance of numerical methods and turbulence models [16-23]. The flow is solved on a cubic domain which spans $[0, 2\pi L]$ in x,y,z coordinate direction, with an initial flow field given by:

$$\begin{aligned} u(t_0) &= V_0 \sin(x/L) \cos(y/L) \cos(z/L) \\ v(t_0) &= V_0 \cos(x/L) \sin(y/L) \cos(z/L) \\ w(t_0) &= 0.0 \\ p(t_0) &= p_0 + \frac{\rho_0 V_0^2}{16} \left[\cos\left(\frac{2x}{L}\right) + \cos\left(\frac{2y}{L}\right) \right] \left[\cos\left(\frac{2z}{L}\right) + 2 \right] \end{aligned} \quad (1)$$

The flow is assumed compressible, and the Reynolds number is defined as $Re = \frac{\rho V_0 L}{\mu}$, where μ is the dynamic viscosity. For the two turbulence models (LBM-VLES and LBM-RANS) studied, a Reynolds number of 1600 was chosen and three resolutions: $128 \times 128 \times 128$, $256 \times 256 \times 256$ and $512 \times 512 \times 512$ were used to study the effects of grid resolution, the results from turbulence simulations are then compared against a LBM-DNS one performed at a resolution of $512 \times 512 \times 512$. For Reynolds number 1×10^6 , the simulations were performed only with LBM-VLES and LBM-RANS, since a DNS simulation at such high Re is not feasible. In all the LBM simulations, a simulation Mach number of 0.1 is used.

3 The Numerical algorithm

3.1 The Lattice Boltzmann Methods

The lattice Boltzmann equation has the following form:

$$f_i(\vec{x} + \vec{c}_i \Delta t, t + \Delta t) - f_i(\vec{x}, t) = C_i(\vec{x}, t) \quad (2)$$

where f_i is the distribution function for particles moving in the i th direction, according to a finite set of the discrete velocity vectors $\{\vec{c}_i : i = 0, \dots, b\}$. $\vec{c}_i \Delta t$ and Δt are space and time increments respectively. For convenience, we choose the convention $\Delta t = 1$ in the subsequent discussions. The collision term on the right hand side of Eq. (2) adopts the simplest and also the most popular form known as the Bhatnagar-Gross-Krook (BGK) form [3, 8, 24]:

$$C_i(\vec{x}, t) = -\frac{1}{\tau} [f_i(\vec{x}, t) - f_i^{eq}(\vec{x}, t)] \quad (3)$$

Here τ is the single relaxation time parameter, and f_i^{eq} is the local equilibrium distribution function, which depends on local hydrodynamic properties [3, 4, 8]. On the other hand, an extension of the Hermite "filtered" collision operator can be applied [26, 27] to enhance numerical stability and symmetry. In the current study, a regularized collision procedure is calculated using the non-equilibrium

distributions $f'_i(\mathbf{x}, t) = \Phi : \Pi$, where Φ is a regularization operator that uses Hermite polynomials and Π is the non-equilibrium part of the momentum flux. The basic concept of regularized collision procedure can be found in [26, 27].

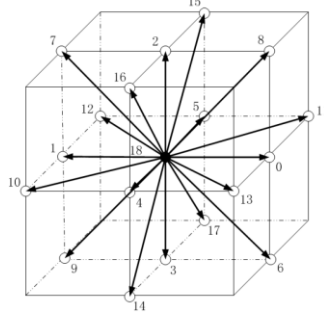


Figure 1. D3Q19 Model.

The basic hydrodynamic quantities, such as fluid density ρ and velocity \bar{u} , are obtained through moment summations; i.e.

$$\rho(\bar{x}, t) = \sum_i f_i(\bar{x}, t), \quad \rho \bar{u}(\bar{x}, t) = \sum_i \bar{c}_i f_i(\bar{x}, t) \quad (4)$$

The three-dimensional D3Q19 model[3, 8] shown in figure 2 is used in the present three-dimensional study to represent the possible velocity directions. The local equilibrium distribution function f_i^{eq} takes the following form so that the recovered macroscopic hydrodynamics satisfy the conservation laws and the leading order resulting macroscopic equations are Galilean invariant at low Mach number[3, 8].

$$f_i^{eq} = \rho w_i \left[1 + \frac{\bar{c}_i \cdot \bar{u}}{T} + \frac{(\bar{c}_i \cdot \bar{u})^2}{2T^2} - \frac{\bar{u}^2}{2T} + \frac{(\bar{c}_i \cdot \bar{u})^3}{6T^3} - \frac{\bar{c}_i \cdot \bar{u}}{2T^2} \bar{u}^2 \right] \quad (5)$$

where w_i are weighting parameters:

$$w_i = \begin{cases} 1/18, & \text{in 6 coordinate directions;} \\ 1/36, & \text{in 12 bi-diagonal directions;} \\ 1/3, & \text{rest particles} \end{cases} \quad (6)$$

and T is the lattice temperature which is generally set to $1/3$ for isothermal simulations.

In the low frequency and long-wave-length limit, one can recover the Navier-Stokes equations through Chapman-Enskog expansion. The resulting equation of state obeys the thermally perfect gas law, $p = \rho T$. The kinematic viscosity of the fluid is related to the relaxation time parameter, τ , by[3, 8, 24]

$$\nu_0 = (\tau - 1/2)T \quad (7)$$

The combination of Eq. (2) to Eq. (7) forms our LBM scheme (LBM momentum solver) for fluid dynamics.

3.1 Fluid Turbulence Model

In order to model the turbulent fluctuations, the LBE is extended by replacing its molecular relaxation time scale with an effective turbulent relaxation time scale; i.e., $\tau \rightarrow \tau_{eff}$, where τ_{eff} can be derived from a systematic renormalization group (RG) procedure[6] as

$$\tau_{eff} = \tau + C_\mu \frac{k^2 / \varepsilon}{T(1 + \tilde{\eta}^2)^{1/2}} \quad (8)$$

where $\tilde{\eta}$ is a combination of a local strain parameter ($\eta = k|S|/\varepsilon$), local vorticity parameter ($\eta_\omega = k|\Omega|/\varepsilon$), and local helicity parameters.

A modified $k-\varepsilon$ two-equation model based on the original RG formulation describes the subgrid turbulence contributions [6, 27, 28, 29], and is given by

$$\begin{aligned}\rho \frac{Dk}{Dt} &= \frac{\partial}{\partial x_j} \left[\left(\frac{\rho v_0}{\sigma_{k_0}} + \frac{\rho v_T}{\sigma_{k_T}} \right) \frac{\partial k}{\partial x_j} \right] + \tau_{ij} S_{ij} - \rho \varepsilon \\ \rho \frac{D\varepsilon}{Dt} &= \frac{\partial}{\partial x_j} \left[\left(\frac{\rho v_0}{\sigma_{\varepsilon_0}} + \frac{\rho v_T}{\sigma_{\varepsilon_T}} \right) \frac{\partial \varepsilon}{\partial x_j} \right] + C_{\varepsilon_1} \frac{\varepsilon}{k} \tau_{ij} S_{ij} - \left[C_{\varepsilon_2} + C_\mu \frac{\tilde{\eta}^3 (1 - \tilde{\eta}/\eta_0)}{1 + \beta \tilde{\eta}^3} \right] \rho \frac{\varepsilon^2}{k}\end{aligned}\quad (9)$$

The parameter $v_T = C_\mu k^2 / \varepsilon$ is the eddy viscosity in the RG formulation. All dimensionless coefficients are the same as in the original models [28, 29].

This LBM-VLES based description of turbulent fluctuation carries flow history and upstream information, and contains high order terms to account for the nonlinearity of the Reynolds stress [6, 10]. This model has unique features to excite the explicit small scale eddies via strong dynamic interactions between the large scale resolved motions and small scale unresolved turbulence, thus creates a broad range energy cascading between the two distinct turbulence spectrums. The LBM-VLES model has been successfully implemented into the state-of-the-art high-fidelity CFD solver SIMULIA PowerFLOW[®] and its accuracy and performance have been extensively validated over a wide range of complex flow problems from aerodynamics, aeroacoustics, to heat transfer in automotive and aerospace industries [12-15]. In the LBM-RANS/URANS approach, large-scale coherent flow structures are resolved, while the effects of small scales turbulence are modeled via a Boussinesq eddy-viscosity approximation with two transport equations from extended renormalization-group theory [28, 29]. This is achieved by setting the effective turbulence viscosity directly equivalent to the eddy viscosity obtained from RG linear eddy viscosity model (equation 9).

4 Results and Discussions

For the Reynolds number of 1600, figure 2 shows the evolution of simulated flow structures (identified through λ_2 criterion [30]) at different instances of time t^* of 6, 9 and 12, with a grid resolution of $512 \times 512 \times 512$. Here t^* is a time scale defined as $t^* = V_0 t / L$. All the simulations predicted that the initially well-defined flow field gradually evolves from “inviscid” like field into a one that being stretched by large vortex structures, the large vortices then breakdown into smaller vortices then cascaded into even smaller ones, and finally forms a near-isotropic state. Apparently, by comparing the results from LBM-VLES and LBM-RANS/URANS, LBM-RANS/URANS appears to be very dissipative and it damped out most of the small-scale structures as the flow transitions to turbulence even when run at such a fine resolution as the LBM-DNS one. On the contrary, LBM-VLES shows predicted flow structures nearly identical to LBM-DNS, this indicates that LBM-VLES can preserves most of the small-scales associated with turbulence.

The evolution of kinetic energy decay is shown in figure 3. Here both the LBM-VLES (figure 2a) and LBM-RANS/URANS (figure 2b) are compared against LBM-DNS results as well as the DNS results from Van Rees et al. [31]. First, the current LBM-DNS result is in excellent agreement with the one from spectral method [31] at same grid resolution. Second, it is evident that LBM-VLES shows good resolution convergence and predicts results, which are very close to LBM-DNS. Finally, LBM-URANS predicts an incorrect trend for the kinetic energy decay, mainly due to a lack of proper energy transferring mechanism from large-scale structures to small-scale structures.

Figure 4 shows the 3D energy spectra measured at different time intervals. Compared with the reference DNS solutions, at all instances of time the predictions of LBM-VLES are far superior over the ones from LBM-RANS/URANS. At $t^* = 12$, the classic Kolmogorov’s $-5/3$ power law in the inertial

subrange is well captured by LBM-VLES, indicating that the LBM-VLES approach can correctly model the energy cascading from larger scales to smaller scales. It should be noted that, at higher wave numbers (>200), the LBM-VLES simulation with a resolution of $512 \times 512 \times 512$ predicted a slightly higher wave spectra than the DNS one, this will need further investigations.

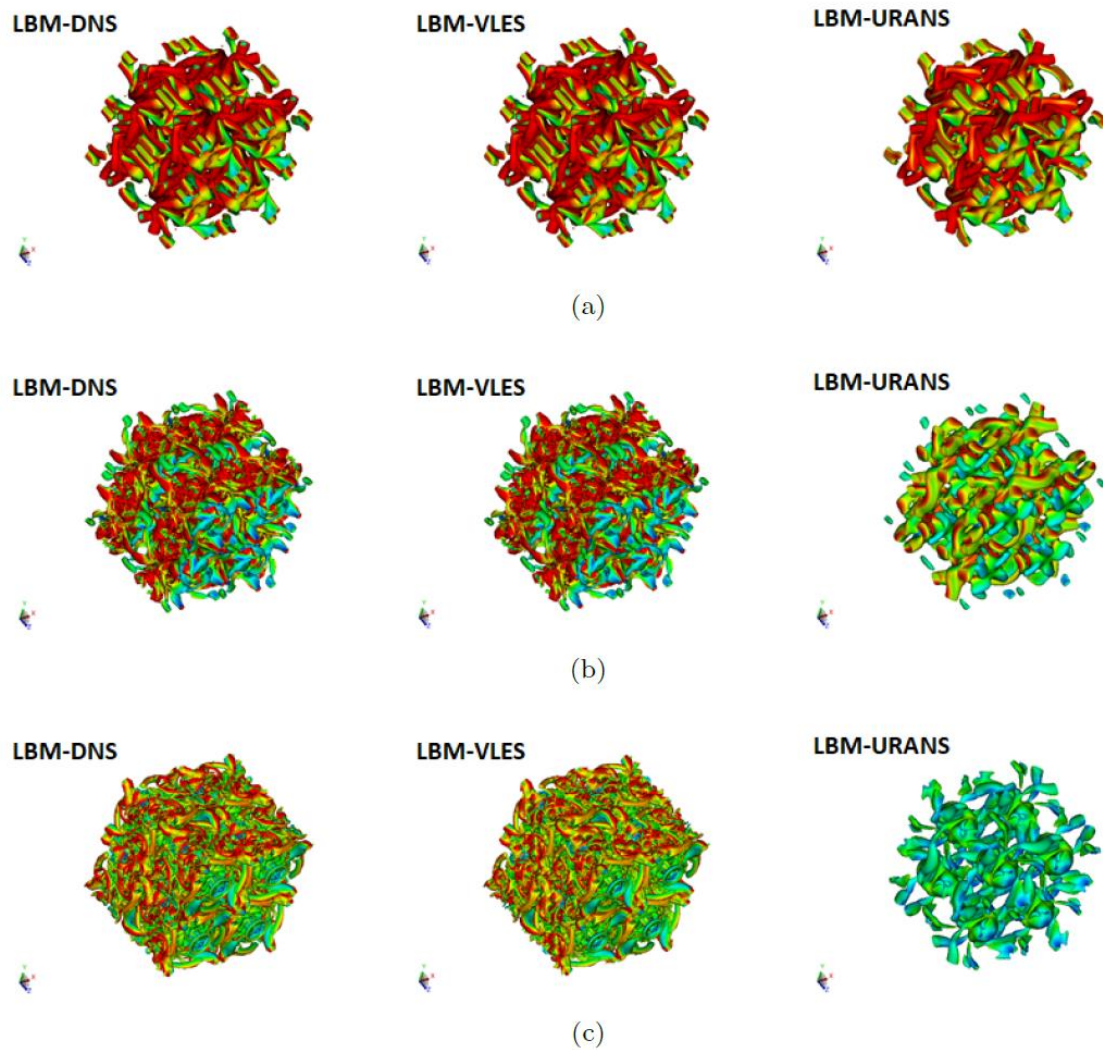


Figure 2. Comparison of flow structures between LBM-DNS, LBM-VLES and LBM-URANS at Reynolds number 1600 and resolution $512 \times 512 \times 512$: (a) $t^* = 6$. (b) $t^* = 9$. (c) $t^* = 12$.

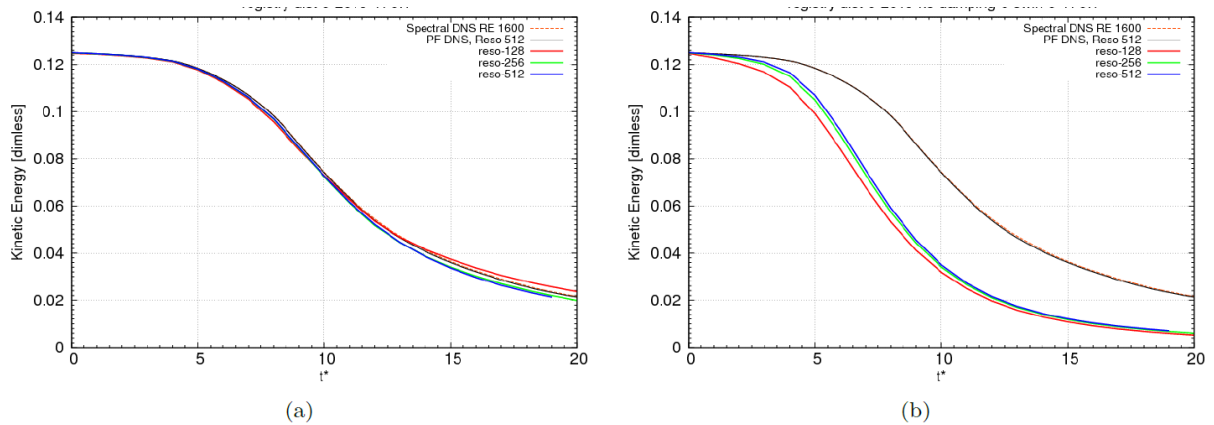


Figure 3. Decay of kinetic energy at Reynolds number 1600. (a) LBM-VLES. (b) LBM-RANS/URANS.

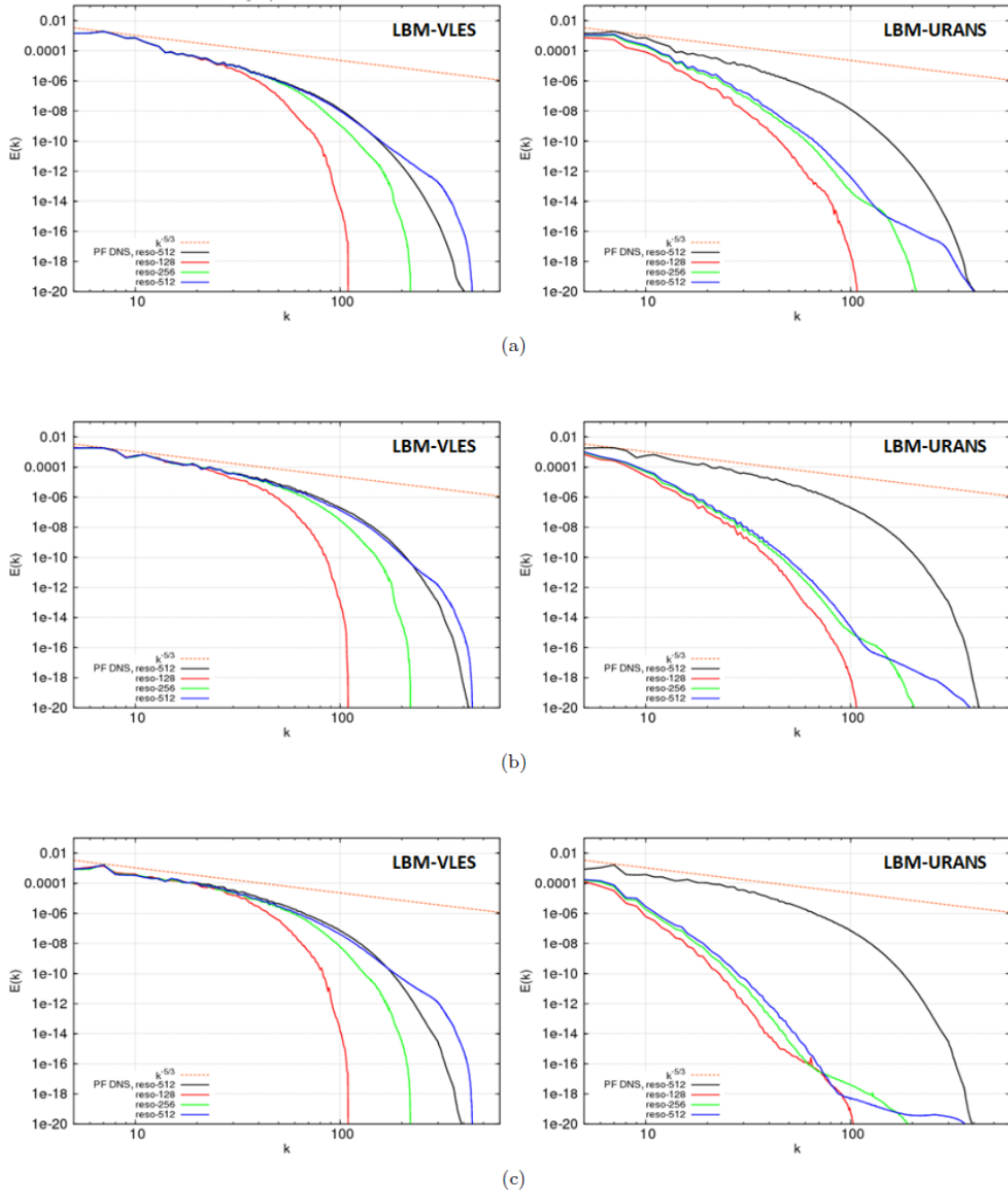


Figure 4. 3D energy spectra at Reynolds number 1600 and (a) $t^* = 6$ (b) $t^* = 9$ (c) $t^* = 12$.

Additional simulations were performed for the TGV problem at a Reynolds number 1×10^6 , such Reynolds number is too high to perform a feasible DNS study, so the simulations are only done with the two turbulence models (LBM-VLES and LBM-RANS/URANS). In figure 5 it is shown that LBM-VLES is still able to capture the right scaling laws in the inertial range, while LBM-RANS/URANS is unable to do so. This confirms the validity of LBM-VLES approach for highly unsteady turbulent flow predictions.

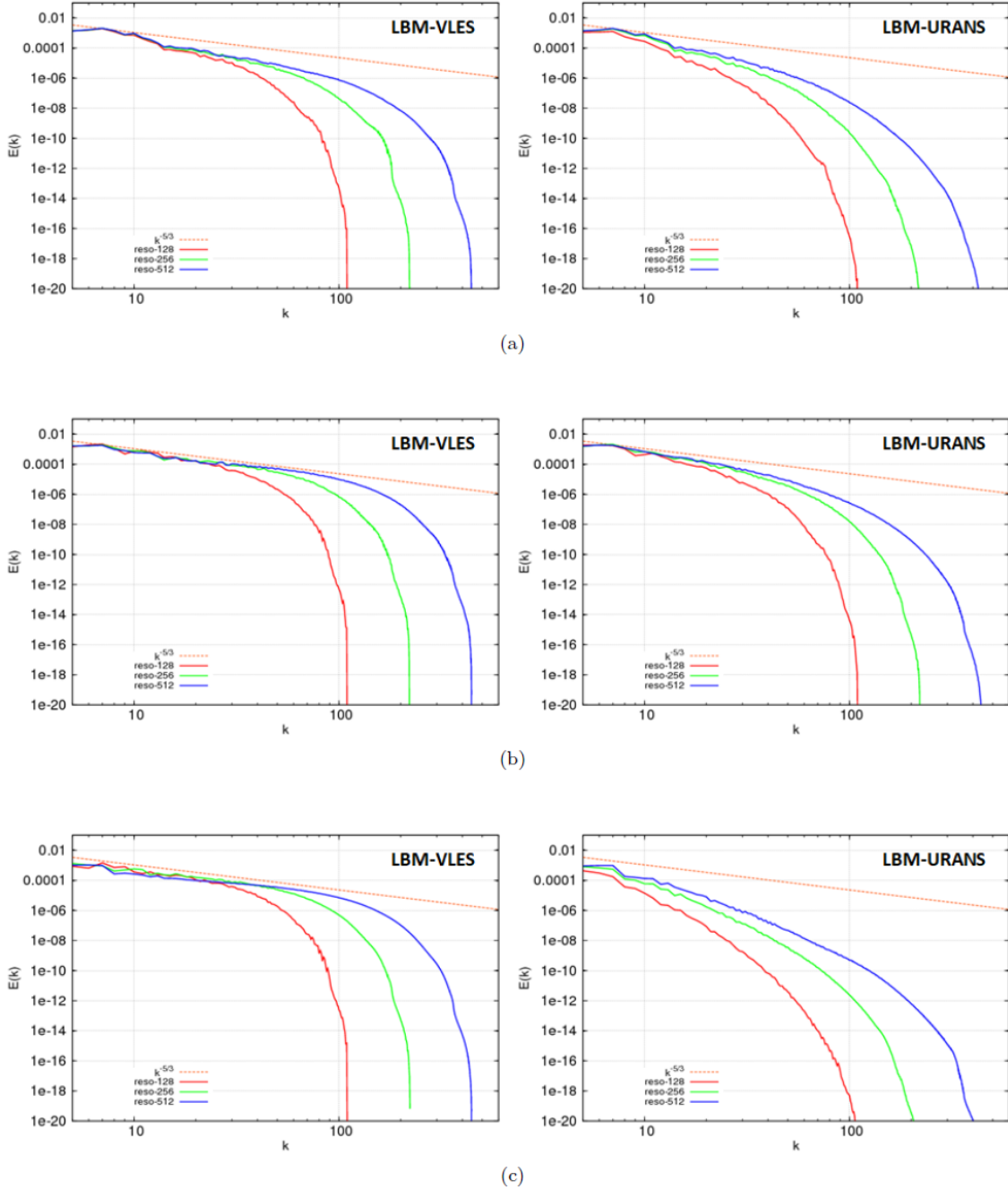


Figure 5. 3D energy spectra at Reynolds number 1×10^6 and (a) $t^* = 6$ (b) $t^* = 9$ (c) $t^* = 12$.

5 Conclusion

We presented the study of three-dimensional Taylor Green Vortex flow problem by two turbulence-modeling approaches: the LBM-RANS/URANS approach and LBM-VLES approach. In the LBM-RANS/URANS (Reynolds-Averaged Navier Stokes) approach, large scale coherent flow structures are resolved, while the effects of small scales turbulence are modeled via a Boussinesq eddy-viscosity approximation with two transport equations from extended renormalization-group theory. In the LBM-VLES (Very Large Eddy Simulation) approach, explicit small scale eddies are excited by strong dynamic interactions between the large scale resolved motions and small scale unresolved turbulence, which creates a broad range energy cascading between the two distinct turbulence spectrums. The simulation results show that LBM-VLES is able to capture to correct kinetic energy decay, can predict the right turbulent structures and recover the classic Kolmogorov's $-5/3$ power scaling laws for the

inertial range, while LBM-RANS/URANS approach gives over-damped predictions. This confirms the validity of the LBM-VLES approach for highly unsteady complex turbulent flow predictions.

References

- [1] Pope, S. B. "Turbulent Flows," Cambridge University Press, 2001.
- [2] Davidson, L. "Fluid mechanics, turbulent flow and turbulence modeling." Chalmers University of Technology, Goteborg, Sweden (Nov 2011) (2018).
- [3] Chen, H., Chen, S., and Matthaeus, W. H., "Recovery of the Navier-Stokes equations using a lattice-gas Boltzmann method," *Physical Review A*, Vol. 45, No. 8, 1992, pp. R5339.
- [4] Chen, S. and Doolen, G. D., "Lattice Boltzmann method for fluid flows," *Annual review of fluid mechanics*, Vol. 30, No. 1, 1998, pp. 329–364.
- [5] Succi, S., *The Lattice Boltzmann equation: For fluid dynamics and beyond*, Oxford university press, 2001.
- [6] Chen, H., Kandasamy, S., Orszag, S., Shock, R., Succi, S., and Yakhot, V., "Extended Boltzmann kinetic equation for turbulent flows," *Science*, Vol. 301, No. 5633, 2003, pp. 633–636.
- [7] Shan, X., Yuan, X.-F., and Chen, H., "Kinetic theory representation of hydrodynamics: A way beyond the Navier–Stokes equation," *Journal of Fluid Mechanics*, Vol. 550, 2006, pp. 413–441.
- [8] Qian, Y., d'Humieres, D. and Lallemand, P., "Lattice BGK Models for the Navier-Stokes Equation," *Europhys. Lett.*, Vol. 17, 1992, pp. 479–484.
- [9] Chen, H., Teixeira, C., and Molvig, K., "Realization of Fluid Boundary Conditions via Discrete Boltzmann Dynamics," *Int. J. Mod. Phys. C*, Vol. 9, 1998, pp. 1281–1292.
- [10] Chen, H., Orszag, S., Staroselsky, I., and Succi, S., "Expanded Analogy between Boltzmann Kinetic Theory of Fluid and Turbulence", *J. Fluid Mech.*, Vol. 519, 2004, pp. 307–314.
- [11] Li, Y., Shock, R., Zhang, R. and Chen, H., "Numerical Study of Flow Past an Impulsively Started Cylinder by Lattice Boltzmann Method," *J. Fluid Mech.*, Vol. 519, 2004, pp. 273–300.
- [12] Kotapati, R., Keating, A., Kandasamy, S., Duncan, B., Shock, R., and Chen, H., "The lattice-Boltzmann-VLES Method for automotive fluid dynamics simulation, a review," *Tech. rep.*, SAE Technical Paper, 2009.
- [13] Meskine, M., Pérot, F., Senthoooran, S., Freed, D., Sugiyama, Z., Polidoro, F., and Gautier, S., "High speed train aeroacoustic solution for community noise using Lattice Boltzmann Method," *SIA, Le Mans, France*, 2012.
- [14] Wang, Z., Alajbegovic, A., Han, J., Donley, T., Horrigan, K., Bloch, D., Pell, M., and Holz, A., "Long Term Transient Cooling of Heavy Vehicle Cabin Compartments," *Tech. rep.*, SAE Technical Paper, 2010.
- [15] Singh, D., Konig, B., Fares, E., Murayama, M., Ito, Y., Yokokawa, Y., and Yamamoto, K., "Lattice-Boltzmann simulations of the JAXA JSM high-lift configuration in a wind tunnel," *AIAA Scitech 2019 Forum*, 2019, p. 1333.
- [16] Taylor, G. I. and Green, A. E., "Mechanism of the production of small eddies from large ones," *Proceedings of the Royal Society of London. Series A-Mathematical and Physical Sciences*, Vol. 158, No. 895, 1937, pp. 499–521.
- [17] Orszag, S. A., "Numerical simulation of the Taylor-Green vortex," *Computing Methods in Applied Sciences and Engineering Part 2*, Springer, 1974, pp. 50–64.
- [18] Brachet, M. E., Meiron, D. I., Orszag, S. A., Nickel, B., Morf, R. H., and Frisch, U., "Small-scale structure of the Taylor–Green vortex," *Journal of Fluid Mechanics*, Vol. 130, 1983, pp. 411–452.
- [19] Wang, Z. J., Fidkowski, K., Abgrall, R., Bassi, F., Caraeni, D., Cary, A., Deconinck, H., Hartmann, R., Hillewaert, K., Huynh, H. T., et al., "High-order CFD methods: current status and

- perspective,” *International Journal for Numerical Methods in Fluids*, Vol. 72, No. 8, 2013, pp. 811–845.
- [20] DeBonis, J., “Solutions of the Taylor-Green vortex problem using high-resolution explicit finite difference methods,” *51st AIAA Aerospace Sciences Meeting including the New Horizons Forum and Aerospace Exposition*, 2013, p. 382.
- [21] Bull, J. R. and Jameson, A., “Simulation of the Taylor–Green vortex using high-order flux reconstruction schemes,” *AIAA Journal*, Vol. 53, No. 9, 2015, pp. 2750–2761.
- [22] Berselli, L. C., “On the large eddy simulation of the Taylor–Green vortex,” *Journal of Mathematical Fluid Mechanics*, Vol. 7, No. 2, 2005, pp. S164–S191.
- [23] Fauconnier, D., De Langhe, C., and Dick, E., “Construction of explicit and implicit dynamic finite difference schemes and application to the large-eddy simulation of the Taylor–Green vortex,” *Journal of Computational Physics*, Vol. 228, No. 21, 2009, pp. 8053–8084.
- [24] Bhatnagar, P., Gross, E. and Krook, M., “A Model for Collision Processes in Gases. I. Small Amplitude Processes in Charged and Neutral One-component System,” *Phys. Rev.*, Vol. 94, 1954, pp. 511-525.
- [25] Chen H, Zhang R, Staroselsky I, Jhon M. Recovery of full rotational invariance in lattice Boltzmann formulations for high Knudsen number flows. *Physica A: Statistical Mechanics and its Applications*. 2006 Mar 15;362(1):125-31.
- [26] Chen, Hudong, Raoyang Zhang, and Pradeep Gopalakrishnan. "Filtered lattice Boltzmann collision formulation enforcing isotropy and Galilean invariance." *Physica Scripta* 95, no. 3 (2020): 034003.
- [27] Yakhot, V. and Orszag, S. A., “Renormalization group analysis of turbulence. I. Basic theory,” *Journal of scientific computing*, Vol. 1, No. 1, 1986, pp. 3–51.
- [28] Yakhot, Victor, and Leslie M. Smith. "The renormalization group, the ϵ -expansion and derivation of turbulence models." *Journal of scientific computing* 7, no. 1 (1992): 35-61.
- [29] Yakhot, V. S. A. S. T. B. C. G., S. A. Orszag, Siva Thangam, T. B. Gatski, and CG1167781 Speziale. "Development of turbulence models for shear flows by a double expansion technique." *Physics of Fluids A: Fluid Dynamics* 4, no. 7 (1992): 1510-1520.
- [30] Jeong, J. and Hussain, F., “On the identification of a vortex,” *Journal of fluid mechanics*, Vol. 285, 1995, pp. 69–94.
- [31] Van Rees, W. M., Leonard, A., Pullin, D. I., and Koumoutsakos, P., “A comparison of vortex and pseudo-spectral methods for the simulation of periodic vortical flows at high Reynolds numbers,” *Journal of Computational Physics*, Vol. 230, No. 8, 2011, pp. 2794–2805.